Chinese Chemical Letters 34 (2023) 108081

Contents lists available at ScienceDirect

Chinese Chemical Letters

journal homepage: www.elsevier.com/locate/cclet

Construction and application of the polyelectrolyte-based sequential artificial light-harvesting system

Chaoqun Ma[a], Ning Han[b,*], Ying Wang[a], Hui Liu[a], Rongzhou Wang[a], Shengsheng Yu[a], Yuebo Wang[a,*], Lingbao Xing[a,*]

[a] School of Chemistry and Chemical Engineering, Shandong University of Technology, Zibo 255000, China
[b] Department of Materials Engineering, KU Leuven, Leuven 3001, Belgium

ARTICLE INFO

Article history:
Received 8 October 2022
Revised 15 December 2022
Accepted 15 December 2022
Available online 18 December 2022

Keywords:
Supramolecular assembly
Light-harvesting system
Electrostatic interaction
Energy transfer
Photocatalysis

ABSTRACT

In this work, we have designed and synthesized a cyano-substituted p-phenylenevinylene derivative (PPTA), which can self-assemble into positively charged nanoparticles in an aqueous solution with a deep green fluorescence. An anionic polyelectrolyte material guar gum modified by carboxylic acid (GP5A) was chosen to build an artificial light-harvesting system (LHS) through self-assembly with PPTA, in which two acceptors Eosin Y (EY) and Nile red (NiR) were loaded into the PPTA-GP5A assemblies through electrostatic interaction and Van der Waals force. By adjusting the molar ratio of PPTA-GP5A/EY at 1:0.004, the one-step artificial LHS can exhibit high energy transfer efficiency (Φ_{ET}) (38.9%) and antenna effect (AE) (4.6). Subsequently, with the addition of NiR, the Φ_{ET} and AE of the two-step sequential artificial LHS were calculated to be 71.9% and 13.5, respectively. Moreover, the two-step artificial LHS constructed by the polyelectrolyte material GP5A can be used as a nanoreactor to photocatalyst alkylation of C-H bonds of phenyl vinyl sulfone (PVS) and tetrahydrofuran (THF) in water with a yield of 42%. Therefore, we have constructed an artificial LHS with two-step energy transfer based on polyelectrolytes through the electrostatic interaction to improve energy transfer efficiency, which can also be used as a nanoreactor for photocatalysis.

Green plants convert solar energy into chemical energy by using various light-harvesting systems (LHSs) contained in them through photosynthesis under sunlight [1]. Inspired by nature, scientists have constructed various artificial LHSs based on noncovalent interactions such as organic nanocrystals [2–4], hydrogen bonding [5–9], coordination interaction [10–14], host-guest interaction [15–23], and electrostatic interaction [24–26] in the process of investigating photosynthesis. For example, Liu *et al.* reported an efficient artificial light-harvesting system based on sulfato-β-cyclodextrin (SCD), an oligo(phenylenevinylene) derivative (OPV-I), and a fluorescent dye, Nile red (NiR), *via* noncovalent interactions in an aqueous solution [20]. Wang *et al.* constructed highly efficient LHSs based on the supramolecular self-assembly of a water-soluble pillar[6]arene (WP6), a salicylaldehyde azine derivative (G), and two different fluorescence dyes, Nile Red (NiR) or Eosin Y (EY) [21]. However, the modification process of fluorescent molecules often requires multi-step, complex synthesis processes and characterization methods. Meanwhile, natural LHSs related photosynthesis not only had a one-step energy transfer process but also often had a two-step or even multi-stage energy transfer process. Although the sequential energy transfer of LHSs based on supramolecular assembly strategy has been reported [27–34], how to construct LHSs that can realize multi-step sequential energy transfer without complex synthesis to realize the simulation of natural photosynthesis is crucial.

Recently, Liu *et al.* constructed efficient artificial LHSs based on a ternary supramolecular system by acrylamide polymers with different 4-phenylpyridium derivatives and macrocyclic compound CB[7] to realize the ultralong delayed fluorescence emissions of dye molecules through effectively energy transfer [35]. Yang *et al.* reported a universal strategy of stepwise Förster resonance energy transfer (FRET) between NiR and Cyanine 7 for a bright near-infrared system with remarkable persistent luminescence in the poly(vinyl alcohol) (PVA) matrix [36]. George *et al.* demonstrated a long-lived phosphor as the energy donor and commercially available fluorescent dyes as the energy acceptor to realize FRET between donor and acceptor chromophores in an amorphous PVA polymer matrix [37]. Therefore, it is very promising to construct

* Corresponding authors.
E-mail addresses: ning.han@kuleuven.be (N. Han), ybwang@sdut.edu.cn (Y. Wang), lbxing@sdut.edu.cn (L. Xing).

https://doi.org/10.1016/j.cclet.2022.108081
1001-8417/

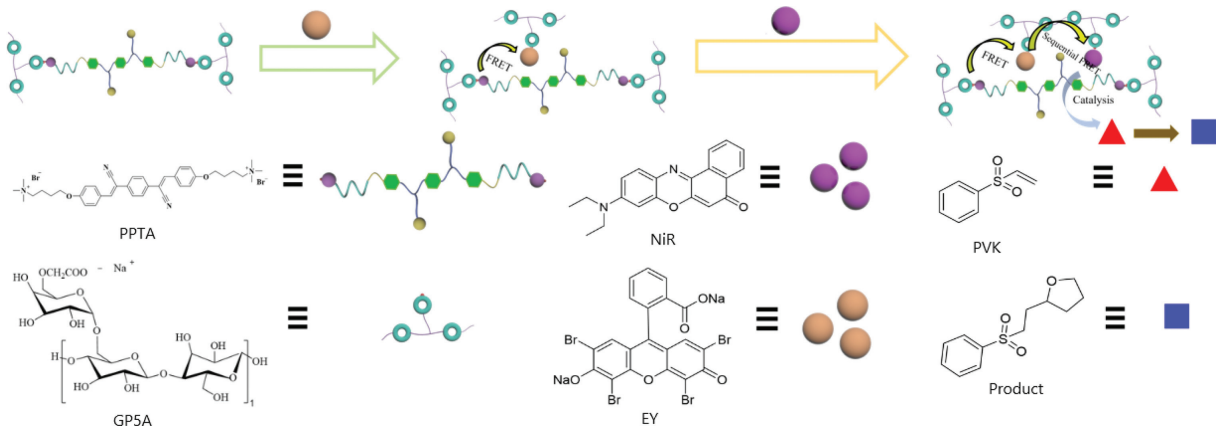

Scheme 1. Illustration of the self-assembly of polyelectrolyte material (GP5A)-based aqueous artificial LHS with sequential energy transfer.

artificial LHSs using a polymer framework to achieve efficient energy transfer.

On the basis of realizing efficient energy transfer, another problem of artificial LHSs is how to convert the captured energy into chemical energy to realize efficient utilization. Up to now, scientists have successfully reported several artificial LHSs that can convert light energy into chemical energy and apply them to photocatalytic organic reactions such as dehalogenation of α-bromoacetophenone [38–44], cross dehydrogenation coupling (CDC) reaction [45–47], photooxidation reaction of sulfide [48,49], C-H arylation of heteroarenes and cross-coupling hydrogen evolution [12], oxidative cyclization [50], alkylation of C—H bonds [51] and so on. However, it is rarely reported that the artificial LHSs with sequential energy transfer can be constructed using polymer frameworks and the light energy can be converted into chemical energy and applied in an aqueous photocatalytic system [52].

In the present work, we have constructed an efficient artificial LHS with a two-step sequential energy transfer by using PPTA-GP5A assembly as energy donors, two dyes EY and NiR as acceptors, in which the positively charged cyano-substituted *p*-phenylenevinylene derivative (PPTA) and negatively charged polyelectrolyte materials GP5A can interact with each other through electrostatic interaction (Scheme 1). The formation of PPTA-GP5A supramolecular assembly was determined by zeta potential test, steady state spectra, and dynamic light scattering (DLS), respectively. Two fluorescent dyes EY and NiR that match the energy level of PPTA-GP5A were selected as energy donors. Driven by the electrostatic interaction, the water-soluble fluorescent dye EY can be easily adsorbed to the quaternary ammonium salt end of the fluorescent molecule PPTA, which greatly shortened the distance between the donor (PPTA-GP5A) and the acceptor (EY), while NiR can be confined in a limited space of GP5A polymers, ensuring the harvested light energy of PPTA-GP5A can be efficiently transferred from PPTA-GP5A to the first acceptor EY, and then to the second acceptor NiR. Moreover, in order to make full use of the harvested solar energy, the constructed artificial LHS with two-step sequential energy transfer based on polyelectrolytes can also be used as a nanoreactor for photochemical catalysis for alkylation of C-H bonds of the phenyl vinyl sulfone (PVS) and tetrahydrofuran (THF) in an aqueous solution (Scheme 1).

PPTA was designed and synthesized through a three-step reaction according to our previous works [41,42]. The identity was confirmed by ^{1}H NMR, ^{13}C NMR and ESI-MS (Supporting information). Unlike many artificial LHSs constructed in the organic phase previously reported, PPTA can be solved in an aqueous solution with an obvious aggregation-induced emission (AIE) phenomenon (Fig. S1 in Supporting information). After the zeta potential test, the results showed that the positive potential was +6.43 mV (Fig. 1a). Then, we chose a polyelectrolyte material anionic guar gum (GP5A), which showed a negative potential of −18.9 mV (Fig. 1b), to construct molecular assembly with PPTA through electrostatic interaction. After that, we tested the zeta potential of the assembled PPTA-GP5A mixed solution, and the result was −3.14 mV (Fig. S2 in Supporting information).

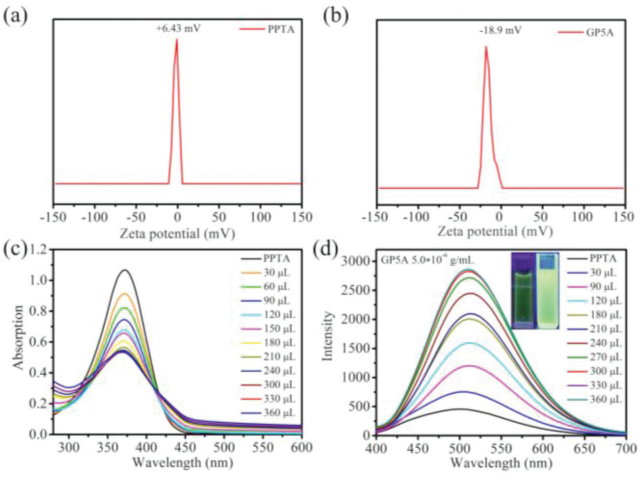

Fig. 1. Zeta potential of PPTA (a) and GP5A (b) in aqueous solution; UV-vis absorption spectra (c) and fluorescence emission spectra (d) of PPTA in aqueous solutions with different concentrations of GP5A. Inset: photograph of PPTA fluorescent color changes before and after addition of GP5A. [PPTA] = 4.0×10^{-5} mol/L, [GP5A] = 5.0×10^{-6} g/mL.

UV–vis absorption and fluorescence emission spectra were carried out to further investigate the interaction between PPTA and GP5A. It can be seen from the UV–vis absorption spectra as shown in Fig. 1c, the absorption of PPTA at 370 nm decreased gradually with the addition of GP5A in the aqueous solution. Meanwhile, the emission of PPTA at 500 nm increased gradually with the addition of GP5A in the aqueous solution (Fig. 1d). When 300 μL GP5A (mass percent of PPTA:GP5A at 60:1) was added into the aqueous solution of PPTA, no more changes could be found in the UV–vis absorption and fluorescence emission spectra (Fig. S3 in Supporting information), indicating the interaction between PPTA and GP5A had reached equilibrium. At this time, the fluorescence quantum yield of PPTA-GP5A assembly was 2.2%. Furthermore, the obvious enhancement of the fluorescence of PPTA-GP5A can be attributed to the electrostatic interaction between the carboxyl anion on the

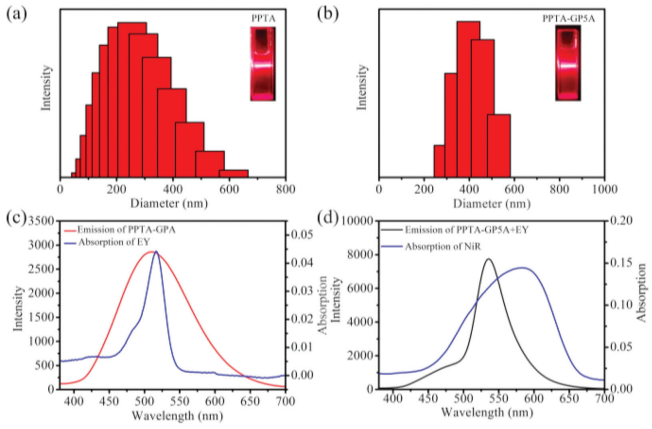

Fig. 2. Particle size distribution of PPTA aqueous solutions before (a) and after (b) adding GP5A. Inset: Tyndall effect of the solution; (c, d) The UV-vis absorption spectra of EY and NiR, and the fluorescence emission spectra ($\lambda_{ex}=370$ nm) of PPTA-GP5A and PPTA-GP5A+EY. [PPTA] = 4.0×10^{-5} mol/L, [GP5A] = 5.0×10^{-6} g/mL, [EY] = 6.0×10^{-6} mol/L, [NiR] = 6.0×10^{-6} mol/L.

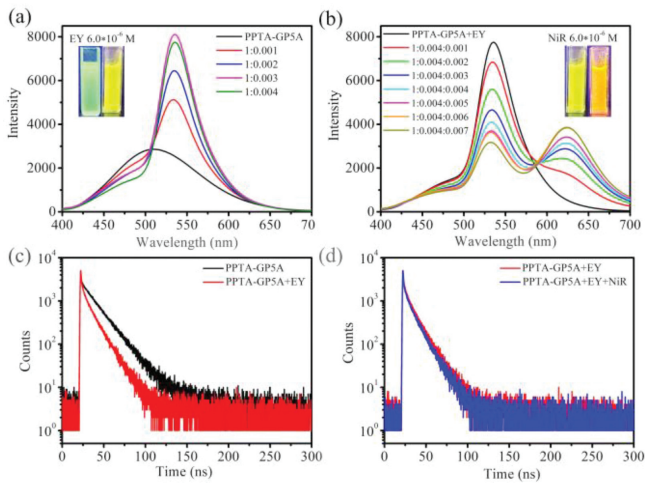

Fig. 3. (a) Fluorescence emission spectra changes of PPTA-GP5A with addition of EY in aqueous solution. Inset: Fluorescent color changes of PPTA-GP5A before and after addition of EY. (b) Fluorescence emission spectra changes of PPTA-GP5A+EY with addition of NiR in aqueous solution. Inset: Fluorescent color changes of PPTA-GP5A+EY before and after addition of NiR. (c) Fluorescence decay profiles of PPTA-GP5A before and after the addition of EY. (d) Fluorescence decay profiles of PPTA-GP5A+EY before and after the addition of NiR. [PPTA] = 4.0×10^{-5} mol/L, [GP5A] = 5.0×10^{-6} g/mL, [EY] = 6.0×10^{-6} mol/L, [NiR] = 6.0×10^{-6} mol/L.

modified GP5A and the quaternary ammonium salt cation on PPTA, in which the vibration and rotation within the molecules can be effectively suppressed. Meanwhile, the fluorescent colors can be changed from deep green for PPTA to light green for PPTA-GP5A in an aqueous solution.

Dynamic light scattering (DLS) experiments can be used to characterize the particle size distribution of PPTA before and after the addition of GP5A. We prepared some mixed solutions of PPTA and PPTA-GP5A, which were completely dissolved by an ultrasonic cleaning machine and studied by DLS. The results showed that the particle size distribution of the PPTA solution without GP5A was mainly centered at about 250 nm (Fig. 2a). When GP5A was added to the PPTA solution, the average particle size of PPTA-GP5A increased to ~400 nm (Fig. 2b). Meanwhile, under the irradiation of a laser lamp, PPTA and PPTA-GP5A both showed an obvious Tyndall effect, indicating the formation of large aggregates. Subsequently, scanning electron microscopy (SEM) and transmission electron microscopy (TEM) were employed to confirm the particles and morphology formed by PPTA and GP5A in the aqueous solution. As shown in Figs. S4a and b (Supporting information), spherical structures can be observed in PPTA before the addition of GP5A, and their diameters are distributed at ~250 nm, consistent with DLS results in Fig. 2a. SEM and TEM experimental results showed that the amorphous structure can be observed when GP5A was added to the aqueous solution of PPTA (Fig. S4), which may be due to the electrostatic interaction between PPTA and GP5A.

Because PPTA-GP5A assemblies exhibit excellent AIE properties in the aqueous solution, which is expected to be used as a good energy donor in LHSs. In order to construct efficiently LHSs, the fluorescent acceptor in the FRET process with matching energy is very important. Therefore, EY was selected as energy acceptors to fabricate LHSs with PPTA-GP5A, because of the good overlap between the absorption band of EY and the fluorescence band of PPTA-GP5A (Fig. 2c), in which the absorption band of EY was 450–550 nm and the emission band of PPTA-GP5A was 450–650 nm. Moreover, the anionic energy acceptors EY can interact with the positively charged energy donors PPTA on the platform of GP5A, in which the transfer distance between the donor PPTA-GP5A and the acceptor EY became closer to benefit for the energy transfer. The above two advantages provided an effective premise for the construction of artificial LHS. When PPTA was excited with a wavelength of 370 nm, the fluorescence emission at 525 nm decreased while the emission at 555 nm increased gradually wtih addition of EY (acceptor) to the aqueous solution of PPTA-GP5A (donor) (Fig. 3a). When the ratio of donor/acceptor was at 1:0.004, the energy transfer efficiency (Φ_{ET}) and antenna effect (AE) of the system reached 38.9% and 4.6 (Figs. S5a and b in Supporting information), while the fluorescence quantum yield was 5.4%. In addition, it can be obviously seen that the color became from light-green to bright yellow of the fluorescence due to the emission of EY when the donor/acceptor ratio up to 1:0.004, indicating the existence of the energy transfer between PPTA and EY (Fig. S6 in Supporting information).

Then, to make the construction of artificial LHS more in line with the process of photosynthesis, we chose the second neutral fluorescent dye NiR as the second acceptors, which had a large spectra overlap with PPTA-GP5A+EY (Fig. 2d). After adding NiR to the PPTA-GP5A+EY solution, the fluorescence intensity of PPTA-GP5A+EY (donor) at 555 nm decreased, while the emission of NiR (the second acceptor) at 620 nm increased gradually (Fig. 3b). When the molar ratio of PPTA-GP5A+EY (donor) and NiR (the second acceptor) was 1:0.004:0.007, Φ_{ET} and AE were calculated to be 71.9% and 13.5 (Figs. S5c and d in Supporting information), while the fluorescence quantum yield was 10.9%. At the same time, under the irradiation of an ultraviolet lamp, the fluorescence colors changed from bright yellow to orange (Fig. S6 in Supporting information), which further proved the successful construction of an efficient artificial LHS with a sequential energy transfer process based on polyelectrolyte materials GP5A. Subsequently, time-resolved fluorescence measurements showed that when the PPTA-GP5A and PPTA-GP5A+EY assemblies (donors) were excited by light with a wavelength of 370 nm, the fluorescence time was significantly shortened from 2.0757 ns to 1.8627 ns, and 1.8627 ns to 1.7640 ns after the addition of the EY (Fig. 3c) and NiR acceptor (Fig. 3d), indicating that the corresponding energy transfer did occur between the donors and acceptors. Then, the Stern-Volmer plots of PPTA-GP5A with different EY and PPTA-GP5A+EY with different NiR concentrations were given in Fig. S7 (Supporting information). The value of K_{SV} for PPTA-GP5A+EY and PPTA-GP5A+EY+NiR are 2.16×10^4 L/mol and 3.98×10^4 L/mol which means that bimolecular quenching occurs between EY or NiR with [PPTA-GP5A]* or [PPTA-GP5A+EY]*.

Table 1
Photocatalysis alkylation of C-H bonds.[a,b]

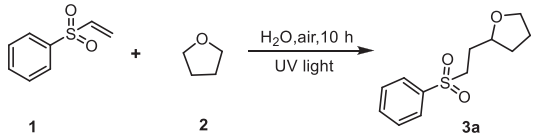

1 2 3a

Entry	Conditions	Light irradiation	Yield (%)[b]
1	None	Yes	no reaction
2	GP5A	Yes	no reaction
3	PPTA	Yes	24
4	EY	Yes	21
5	NiR	Yes	27
6	EY+NiR	Yes	29
7	PPTA-GP5A	Yes	28
8	PPTA-GP5A+EY	Yes	30
9	PPTA-GP5A+EY+NiR	Yes	42
10[c]	PPTA-GP5A+EY+NiR	No	no reaction

[a] Reaction conditions: phenyl vinyl sulfone (16.8 mg, 0.1 mmol), tetrahydrofuran (16.5 μL, 0.2 mmol), PPTA-GP5A+EY+NiR (0.8 mol%) aqueous solution (2 mL), 10 W UV light, room temperature, 10 h.
[b] Isolated yields.
[c] Without a UV light.

To better simulate the process of photosynthesis in nature and make full use of the energy received by the energy acceptor, we used the sequential energy transfer artificial LHS (PPTA-GP5A+EY+NiR) constructed by the polyelectrolyte material GP5A to provide a reaction platform for the alkylation of C-H bonds between phenyl vinyl sulfone (PVS) and tetrahydrofuran (THF) (Fig. S8 in Supporting information). As shown in Table 1, in the presence of 0.8 mol% PPTA-GP5A+EY+NiR (1:0.004:0.007), the yield reached 42% after irradiation with 370 nm light for 10 h. In contrast, under the same conditions, the yields of other systems including PPTA-GP5A, EY+NiR, GP5A, PPTA, PPTA-GP5A+EY, or without any catalyst were lower than 30%. The good catalytic of the PPTA-GP5A+EY+NiR system may be attributed to the encapsulation of dye molecules by PPTA-GP5A assemblies, in which the AIE effect of the donor and the proper arrangement of the dyes in the assemblies, the PPTA-GP5A+EY+NiR can realize an efficient two-step energy transfer process, which greatly improves the light-use efficiency and exhibits optimal photocatalytic efficiency.

Then, we proposed a relatively suitable photocatalysis mechanism for the reaction of PVS and THF. Firstly, the PPTA-GP5A assembly was excited at 370 nm by ultraviolet light in an aqueous solution, and then transformed into an excited state [PPTA-GP5A]*. Subsequently, the assembly in the excited state transfers energy to the acceptor dye EY to form the excited state [EY]*, and further transfers energy to the acceptor dye NiR to form [NiR]*. Raw materials **1** and **2** underwent a single electron transfer reduction (SET) on [NiR]* respectively. The terminal double bond of raw material 1 is opened to generate free radical intermediate state **A**. At the same time, the C-H bond of raw material **2** is broken after obtaining energy to generate free radical intermediate state **B** and hydrogen radicals. Finally, a new bond is formed by the anti-Markovnikov rule of free radical interaction, and the final product is obtained (Fig. S9 in Supporting information).

In summary, we have constructed an artificial light-harvesting system with a two-step sequential energy transfer process based on a polyelectrolyte material (GP5A) through the electrostatic interaction to close the distance between the donors and acceptors to improve energy transfer efficiency by using the AIE molecule PPTA as energy donors, and two fluorescent dyes EY and NiR as energy acceptors in an aqueous solution. The harvested light energy in the sequential energy transfer artificial LHS can be efficiently transferred and further used for the alkylation of C-H bonds between phenyl vinyl sulfone (PVS) and tetrahydrofuran (THF) in water with a yield of 42%. The establishment of this system not only provides a new method for constructing light-harvesting systems with sequential energy transfer systems based on polyelectrolytes; but also provides beneficial exploration for artificial light-harvesting systems to simulate natural photosynthesis and realize the conversion of light energy to chemical energy for photocatalysis.

Declaration of competing interest

The authors declare that they have no known competing financial interests or personal relationships that could have appeared to influence the work reported in this paper.

Acknowledgments

We are grateful for the financial support from the National Natural Science Foundation of China (Nos. 52205210 and 22005179) and the Natural Science Foundation of Shandong Province (Nos. ZR2020MB018, ZR2022QE033, ZR2020QB113 and ZR2018BEE015).

Supplementary materials

Supplementary material associated with this article can be found, in the online version, at doi:10.1016/j.cclet.2022.108081.

References

[1] H.Q. Peng, L.Y. Niu, Y.Z. Chen, et al., Chem. Rev. 115 (2015) 7502–7542.
[2] P.Z. Chen, Y.X. Weng, L.Y. Niu, et al., Angew. Chem. Int. Ed. 55 (2016) 2759–2763.
[3] M.J. Sun, Y. Liu, W. Zeng, et al., J. Am. Chem. Soc. 141 (2019) 6157–6161.
[4] M.J. Sun, Y.W. Zhong, J. Yao, Angew. Chem. Int. Ed. 57 (2018) 7820–7825.
[5] K. Diao, D.J. Whitaker, Z. Huang, et al., Chem. Commun. 58 (2022) 2343–2346.
[6] Y.Z. Ma, H. Xiao, X.F. Yang, et al., J. Phys. Chem. C 120 (2016) 16507–16515.
[7] H.Q. Peng, J.F. Xu, Y.Z. Chen, et al., Chem. Commun. 50 (2014) 1334–1337.
[8] H.Q. Peng, C.L. Sun, L.Y. Niu, et al., Adv. Funct. Mater. 26 (2016) 5483–5489.
[9] X. Zhu, J.X. Wang, L.Y. Niu, et al., Chem. Mater. 31 (2019) 3573–3581.
[10] K. Acharyya, S. Bhattacharyya, H. Sepehrpour, et al., J. Am. Chem. Soc. 141 (2019) 14565–14569.
[11] Y.X. Hu, P.P. Jia, C.W. Zhang, et al., Org. Chem. Front. 8 (2021) 5250–5257.
[12] Z. Zhang, Z. Zhao, Y. Hou, et al., Angew. Chem. Int. Ed. 58 (2019) 8862–8866.
[13] P. Wang, X. Miao, Y. Meng, et al., ACS Appl. Mater. Interfaces 12 (2020) 22630–22639.
[14] C.B. Huang, L. Xu, J.L. Zhu, et al., J. Am. Chem. Soc. 139 (2017) 9459–9462.
[15] H.J. Kim, D.R. Whang, J. Gierschner, et al., Angew. Chem. Int. Ed. 55 (2016) 15915–15919.
[16] P.C. Nandajan, H.J. Kim, S. Casado, et al., J. Phys. Chem. Lett. 9 (2018) 3870–3877.
[17] K. Wang, K. Velmurugan, B. Li, et al., Chem. Commun. 57 (2021) 13641–13654.
[18] T. Xiao, W. Zhong, L. Zhou, et al., Chin. Chem. Lett. 30 (2019) 31–36.
[19] D. Zhang, Y. Liu, Y. Fan, et al., Adv. Funct. Mater. 26 (2016) 7652–7661.
[20] J.J. Li, Y. Chen, J. Yu, et al., Adv. Mater. 29 (2017) 1701905.
[21] S. Guo, Y. Song, Y. He, et al., Angew. Chem. Int. Ed. 57 (2018) 3163–3167.
[22] T.X. Xiao, J. Wang, Y. Shen, et al., Chin. Chem. Lett. 32 (2021) 1377–1380.
[23] C. Peng, W. Liang, J. Ji, et al., Chin. Chem. Lett. 32 (2021) 345–348.
[24] C.Y. Qin, Y. Li, Q.F. Li, C. Yan, L.P. Cao, Chin. Chem. Lett. 32 (2021) 3531–3534.
[25] I. Shulov, S. Oncul, A. Reisch, et al., Nanoscale 7 (2015) 18198–18210.
[26] C. Vijayakumar, K.K. Kartha, B. Balan, et al., J. Phys. Chem. C 123 (2019) 13141–13146.
[27] M. Suresh, A.K. Mandal, E. Suresh, et al., Chem. Sci. 4 (2013) 2380–2386.
[28] Z. Xu, D. Gonzalez-Abradelo, J. Li, et al., Mater. Chem. Front. 1 (2017) 1847–1852.
[29] L. Ji, Y. Sang, G. Ouyang, et al., Angew. Chem. Int. Ed. 58 (2019) 844–848.
[30] J.J. Li, H.Y. Zhang, X.Y. Dai, et al., Chem. Commun. 56 (2020) 5949–5952.
[31] Q. Song, S. Goia, J. Yang, et al., J. Am. Chem. Soc. 143 (2020) 382–389.
[32] G. Sun, W. Qian, J. Jiao, et al., J. Mater. Chem. A 8 (2020) 9590–9596.
[33] T. Xiao, L. Zhang, H. Wu, et al., Chem. Commun. 57 (2021) 5782–5785.
[34] W. Zhang, Y. Luo, X.L. Ni, et al., Chem. Eng. J. 446 (2022) 136954.
[35] W.W. Xu, Y. Chen, Y.L. Lu, et al., Angew. Chem. Int. Ed. 61 (2022) e202115265.
[36] F. Lin, H. Wang, Y. Cao, et al., Adv. Mater. 34 (2022) e2108333.
[37] S. Kuila, S.J. George, Angew. Chem. Int. Ed. 59 (2020) 9393–9397.
[38] M. Hao, G. Sun, M. Zuo, et al., Angew. Chem. Int. Ed. 132 (2020) 10181–10186.
[39] G. Sun, M. Zuo, W. Qian, et al., Green Synth. Catal. 2 (2021) 32–37.
[40] Z. Bai, K. Velmurugan, X. Tian, et al., Beilstein J. Org. Chem. 18 (2022) 429–437.

[41] X.L. Li, Y. Wang, A. Song, et al., Soft Matter 17 (2021) 9871–9875.
[42] X.L. Li, Y. Wang, M.H. Zhang, et al., Dyes Pigments 197 (2022) 109895.
[43] X. Li, Y. Wang, A. Song, et al., Chin. J. Chem. 39 (2021) 2725–2730.
[44] X. Li, S. Yu, Z. Shen, et al., J. Colloid Interface Sci. 617 (2022) 118–128.
[45] W.J. Li, X.Q. Wang, D.Y. Zhang, et al., Angew. Chem. Int. Ed. 60 (2021) 18761–18768.
[46] T. Cai, B. Huang, H. Hu, et al., Dyes Pigments 200 (2022) 110156.
[47] Y. Wang, N. Han, X.L. Li, et al., ACS Appl. Mater. Interfaces 14 (2022) 45734–45741.
[48] P.P. Jia, L. Xu, Y.X. Hu, et al., J. Am. Chem. Soc. 143 (2020) 399–408.
[49] P. Jia, Y. Hu, Z. Zeng, et al., Chin. Chem. Lett. 34 (2023) 107511.
[50] A. Kumar, R. Saha, P.S. Mukherjee, Chem. Sci. 12 (2021) 5319–5329.
[51] D. Zhang, W. Yu, S. Li, et al., J. Am. Chem. Soc. 143 (2021) 1313–1317.
[52] C.Q. Ma, X.L. Li, N. Han, et al., J. Mater. Chem. A 10 (2022) 16390–16395.